Metabolic imaging at the nanoscale with Multi-Isotope Imaging Mass Spectrometry (MIMS)

AUTHOR(S) AND CONTACT INFORMATION:

Derek P. Narendra[1]*, Matthew L. Steinhauser[2]*

1. National Institute of Neurological Disorders and Stroke, National Institutes of Health, Bethesda, MD

E-mail: derek.narendra@nih.gov

Address:

35 Convent Dr.

Bldg. 35, Rm 2A-215

Bethesda, MD 20814

Phone: 301-594-4737

2. Department of Medicine, Aging Institute, University of Pittsburgh School of Medicine, Pittsburgh, PA

E-mail: msteinhauser@pitt.edu

Address:

558 Bridgeside Point
100 Technology Drive
Pittsburgh, PA 15219
Phone: 412-383-0891

* Corresponding authors

This is the author manuscript accepted for publication and has undergone full peer review but has not been through the copyediting, typesetting, pagination and proofreading process, which may lead to differences between this version and the Version of Record. Please cite this article as doi: 10.1002/cpcb.111.

ABSTRACT:

Incorporation of a stable isotope metabolic tracer into cells or tissue can be followed at submicron resolution by Multi-Isotope Imaging Mass Spectrometry (MIMS), a form of imaging secondary ion microscopy optimized for accurate isotope ratio measurement from microvolumes of sample (as small as ~30 nm across). In a metabolic MIMS experiment, a cell or animal is metabolically labelled with a tracer containing a stable isotope. The relative accumulation of the heavy isotope into the fixed sample is then measured as an increase over its natural abundance by MIMS. MIMS has been used to measure protein turnover in single organelles, track cellular division *in vivo*, visualize of sphingolipid rafts on the plasma membrane, and measure dopamine incorporation into dense core vesicles, among other biological applications. In this Current Protocol we introduce metabolic imaging by NanoSIMS, by focusing on two specific applications: quantifying protein turnover in single organelles of cultured cells and tracking cell replication in the mouse tissues *in vivo*. These examples illustrate the versatility of the metabolic imaging with MIMS.

Basic Protocol 1: Metabolic labeling for MIMS

Support Protocol 1: Preparing silicon wafers as sample supports for MIMS (**Basic Protocol 2**)

Basic Protocol 2: Embedding samples for correlative TEM and MIMS with a genetically encoded reporter

Alternative Protocol 1: Embedding samples for correlative light microscopy and MIMS

Basic Protocol 3: Analysis of MIMS data

KEYWORDS:

NanoSIMS

Stable Isotope Labelling in Cell Culture

Fate mapping

INTRODUCTION:

Multi-Isotope Imaging Mass Spectrometry (MIMS) is a form of secondary ion mass spectrometry distinctive for its ability to quantify atomic isotope ratios at a lateral resolution of ~30 - 100 nm (Slodzian et al., 1992). Use of MIMS has expanded over the last decade with the developement of a commercially available instrument called NanoSIMS (Cameca).The objective of a biological MIMS experiment is often to track incorporation of a heavy-isotope labelled metabolite into a biological specimen (Slodzian et al., 1992; Lechene et al., 2006). In a very general sense, imaging such tracers with MIMS is analogous to metabolic imaging by Positron Emission Tomography but at the nano- rather than the meso-scale. MIMS has been used in this way to assess protein turnover in single

organelles, track cellular division *in vivo*, visualize of sphingolipid rafts on the plasma membrane, and measure dopamine incorporation into dense core vesicles, among other applications (Narendra et al., 2020; Steinhauser et al., 2012; Senyo et al., 2013; Frisz et al., 2013; Lovrić et al., 2017; Thomen et al., 2020). Additionally, metabolic labeling with MIMS has been applied to diverse biological systems, from microbes to humans (Lechene et al., 2006; Steinhauser et al., 2012; Guillermier et al., 2017; Lechene et al., 2007).

In preparation for metabolic analysis by MIMS, the cell or organism is metabolically labelled with a tracer containing a stable (i.e., non-radioactive) isotope. The sample is typically fixed, embedded in plastic, and thin sectioned with an ultramicrotome, similar to standard sample preparation for transmission electron microscopy (TEM). Alternatively, the sample may be directly grown or whole-mounted on a support (Lechene et al., 2006; Frisz et al., 2013; Lovrić et al., 2017). The specimen is then placed in the NanoSIMS instrument under strong vacuum. A primary ion source sputters material from the first few atomic layers of the sample surface, forming atomic and poly-atomic secondary ions. If the primary ion source is positive (usually cesium), it produces negatively charged secondary ions; elements such as carbon, hydrogen, nitrogen (as a di-atom with carbon), oxygen, and sulfur are efficiently ionized in this way. Alternatively, if the source in negative (usually oxygen), it produces positively charged ions; this is useful for ionizing elements like calcium and magnesium. Once sputtered, these secondary ions are focused by ion optics into a secondary ion beam and then separated by their *m/z* ratio across a focal plane in the magnetic sector mass spectrometer of the instrument. In its current iteration, the commercial NanoSIMS 50L has seven detectors, each tuned to capture ions of a specific mass. This allows simultaneous acquisition of seven ions – which can be increased to nine ions, using peak switching methods (Guillermier et al., 2014). As the primary beam is rastered across the sample surface, multiple co-registered ion images are generated in parallel, each representing the relative ion abundance in the imaged plane. As MIMS breaks material down to its constitutive atoms, directly measured heavy atoms derived from the metabolic tracer serve as a proxy for the tracer.

Some elements are ionized more efficiently than others and, additionally, ionization can be enhanced or suppressed by the surrounding material. Consequently, measurement of ion abundance from different parts of the specimen is generally semi-quantitative. At any given spot under active analysis, however, isotopes of a single element (e.g., ^{12}C and ^{13}C) are ionized and measured with equal efficiency (Slodzian et al., 1992; Lechene et al., 2006). Thus, when acquired simultaneously, isotope ratio measurements (e.g. $^{13}C/^{12}C$) *are* quantitative. The high accuracy of isotope ratio measurements enables metabolic imaging of stable isotope-labeled tracers by MIMS.

In this Current Protocol we introduce metabolic imaging by MIMS, by focusing on two specific applications: quantifying protein turnover in single organelles of cultured cells and tracking cell replication in mouse tissues *in vivo*. These examples illustrate the versatility of metabolic imaging with MIMS. The article is broken up into five protocols each addressing a key technical step in a complete metabolic MIMS experiment: metabolic labeling for MIMS (**Basic Protocol 1**), preparing silicon wafers as sample supports for MIMS (**Support Protocol 1**), embedding samples for correlative TEM and MIMS with a genetically encoded reporter (**Basic Protocol 2**), alternatively embedding

samples for correlative light microscopy and MIMS **(Alternative Protocol 1)**, and analysis of MIMS data (**Basic Protocol 3**).

BASIC PROTOCOL 1: **Metabolic Labelling for MIMS**

The power of MIMS is its ability to reveal metabolic incorporation of labeled tracer in cells or tissues at submicron resolution. Importantly, though, MIMS directly measures a rare atom in the tracer (often a stable isotope, ^{2}H, ^{13}C, ^{15}N, or ^{18}O) and not the tracer itself. Thus, the rare atom is a proxy for the tracer in much the same way that a peptide is a proxy for a protein in an LC-MS/MS experiment or paired-end read is a proxy for a gene analyzed by Next Generation Sequencing. However, because the atom and not the tracer is measured, different labeled atoms in the tracer may give different results, depending on how the tracer is metabolized *in vivo*. For instance, the ^{2}H in L-serine (3,3-^{2}H, ^{15}N) is incorporated in fatty acids through the one carbon metabolism pathway, whereas ^{15}N is not (Ducker et al., 2016). Thus, the patterns of ^{2}H and ^{15}N incorporation into the sample may appear different by MIMS, even though both labels came from the same parent molecule.

The label detected by MIMS is most often an atom that is rare but not absent in the sample. How well the label is detected depends on several factors: its background abundance (a product of its natural abundance and background concentration), how well it ionizes, and the accuracy with which it is detected. Consider labelling DNA with ^{13}C-thymidine. ^{13}C has a natural abundance of about 1.1% and carbon a concentration of about 0.606 M in an embedded biological specimen (Thomen et al., 2020). Thus, to be detected, ^{13}C in thymidine must exceed the variance of the background ^{13}C measurement. ^{15}N by contrast has a lower natural abundance and lower concentration in the specimen, but still ionizes well (as the $^{12}C^{15}N$ di-atom) and can be measured accurately. Thus, ^{15}N in thymidine is detected with a higher signal to noise ratio (SNR) than is ^{13}C thymidine. Of the commonly used labels, ^{15}N typically has the highest SNR.

^{13}C-tracers, however, have some additional advantages. ^{13}C-tracers are commonly used in metabolic studies of bulk samples, using, e.g., LC-MS/MS and isotope ratio MS (IRMS)-based techniques. As a result, many ^{13}C-labelled tracers are commercially available for use in MIMS. Moreover, the dilution of signal due to the carbon content of plastic embedding media can be viewed as an advantage for some MIMS applications. As recently shown by the Ewing lab, because the ^{13}C concentration in the embedding media (e.g., Epon 812) is a known quantity, it can be used as an internal standard for the absolute quantification of a ^{13}C-containing metabolite embedded within (Thomen et al., 2020). Thus, despite lower SNR, ^{13}C may represent the best stable isotope for some applications.

^{2}H generally results in good SNR but the small mass of its isotope, ^{1}H, prohibits parallel detection of heavier species like $^{12}C^{14}N$, ^{31}P, and ^{32}S by NanoSIMS. This is due to physical constraints of the NanoSIMS 50L magnetic sector, which has an accessible mass range of M_{max}/M_{min}= 21. Thus, species with a mass of greater than approximate 21 cannot be detected in parallel with ^{1}H with the commercially available configuration. An alternative measurement strategy is to use C_2H and C_2D

(with masses of 25 and 26) as proxy elements for H and D (Guillermier et al., 2017b). Mass overlap with other C2 polyatoms, however, reduces the accuracy of ratio quantification, which ultimately lowers its SNR as a label. Additionally, proton exchange between labelled metabolite and water, may deplete signal from some target metabolites and increase background. ^{18}O offers another choice for labeling with low natural abundance, good ionization, and a mass near other elements commonly detected in parallel. Its more wide-spread use, however, has been limited by its expense. In addition, similar to proton exchange with hydrogen, oxygen exchange between labelled metabolites and water may deplete signal from some target metabolites and increase background.

The dynamic range of the label depends not only its SNR but also on how well it is metabolically incorporated into the fixable biomass of the sample. For instance, if a cell has a higher concentration of protein than DNA, the ceiling for ^{15}N incorporation will be higher for a sample maximally labelled with ^{15}N amino acids than one maximally labelled with ^{15}N nucleotides. Practically, the ceiling for ^{15}N-thymidine incorporation into the nucleus of cultured cells is approximately 200% of natural abundance, whereas much higher levels of incorporation (> 1000%) can be achieved labelling nuclear protein with ^{15}N-leucine.

Probes with other elements that are rare in the specimen can also be detected by MIMS. Platinum-based chemotherapeutic drugs, for instance, have been tracked by measurement of ^{194}Pt (Legin et al., 2014). Similarly, drugs or probes containing transition metals such as ^{47}Ag, ^{79}Au, Fe oxides, and Cu oxides can be detected, as can the lanthanide series of 15 elements (^{57}La through ^{71}Lu) (reviewed in (Nuñez et al., 2017)). The utility of the lanthanide series for multiplexed immunolabelling was established using MIMS (with an oxygen source to produce positive ions) and more recently has formed the basis of commercialized SIMS-TOF instruments that can detect >30 antibodies in parallel (Angelo et al., 2014; Keren et al., 2019).

Additionally, halogens, found in many commonly used fluorescent dyes and nucleoside analogs like BrdU, can be detected by MIMS, enabling structural definition or metabolic labeling. The ^{81}Br in BrdU, for instance, has been used to detect DNA replication, and the ^{19}F in Lysotracker red has been used to image acidic organelles such as lysosomes (Steinhauser et al., 2012; Legin et al., 2014). Similarly, ^{35}Cl in MitoTracker dyes such as MitoTracker RED CMXRos could theoretically be used to image mitochondria.

Finally, many commonly used fluorophores are fluorinated, including Oregon Green, the BODIPY series, and the Pacific Dye series. When conjugated to antibodies, oligonucleotides, or other probes, these provide molecular definition in MIMS analyses. This has been demonstrated using *in situ* hybridization probes linked to Oregon Green 488-X (detected as ^{19}F), BODIPY TMR-X (detected as ^{19}F), and 5-carboxy-2',4',5',7'-tetrabromosulfonefluorescein (detected as ^{81}Br). These probes allowed the authors to identify microbes within a consortium that differentially incorporated ^{15}N-dinitogen and ^{13}C-bicarbonate (Behrens et al., 2008).

Materials:

SILAC DMEM High Glucose, lacking L-arginine, L-lysine, L-leucine, and L-methionine (Athena ES cat# 0420)

L-leucine (15N) (Cambridge Isotope Laboratories, cat# NLM-142-PK)

L-methionine (Sigma, cat# M8439)

L-arginine (Sigma, cat# A4474)

FBS, dialyzed (Thermo Scientific, A3382001)

Cycloheximide (Sigma, cat# 239764)

HeLa cells (ATCC, cat# CCL-2)

Note: cycloheximide is toxic and should be handled with appropriate personal protective equipment (PPE) following the manufacturer's SDS.

Metabolic labelling of cells for analysis of bulk protein turnover in individual organelles

Protein can be metabolically labelled using most amino acids. L-leucine (L) has been used most often for assessment of bulk protein turnover, as it is abundant in bulk protein and has high blood levels in mammals. It is also relatively inexpensive. L-arginine (R) and L-lysine (K) are useful alternatives. Like L-leucine they are abundant in bulk protein and mammalian blood, but in addition, their incorporation into tryptic peptides is easily measured by LC-MS/MS as an orthogonal method. Because trypsin cleaves after R and K, there is only one R/K residue in each tryptic peptide. The ^{15}N-containing amino acids most commonly used for SILAC are R4 (15N4) and K8 (13C6; 15N2). Of these K8 is typically the least expensive. K2 (15N2) is also available, but analysis of LC-MS/MS data may require deconvolution of isotopic peaks, necessitating more specialized workflows. As noted above, ^{15}N has higher SNR than ^{13}C. Thus, we prefer ^{15}N-labelled amino acids for NanoSIMS, but ^{13}C-labelled amino acids have also been used.

1. To make ^{15}N-L-leucine DMEM, add 105 mg/L of ^{15}N-L-leucine to SILAC DMEM. Supplement with unlabeled arginine (84 mg/L), lysine (146 mg/L), and methionine (149 mg/L), and add dialyzed FBS to a final concentration of 10%. *To maximize the signal, ideally the labeled metabolite is introduced into tissue culture media lacking the metabolite. Depending on the cell line and metabolite, however, this may not be possible. In this case the labeled metabolite can be added to complete media, but the signal will be diluted by the unlabeled metabolite in the media.*
2. As a control experiment, incubate the HeLa cell line in ^{15}N-L-leucine DMEM for 8 hrs in the presence or absence of 100 μM cycloheximide (CHX). *CHX blocks protein translation. If an*

increase in $^{12}C^{15}N$ signal over natural abundance reflects ^{15}N incorporation into bulk protein, the increase will be inhibited by CHX.

3. For pulse experiments, incubate the HeLa cell line in ^{15}N-L-leucine DMEM for 24 hrs. *Incorporation into bulk protein is approximately 30% after 8 hrs and 70% after 24 hrs in HeLa cells. The $^{15}N/^{14}N$ ratio is ~500% greater than natural abundance after a 24 hr pulse in HeLa cells.*
4. For chase experiments, incubate the HeLa cell line ^{15}N-L-leucine DMEM until it is >95% labelled (achieved after 5 cell doublings). Heavy media is then exchanged for light media and the heavy amino acid is chased for 24 hrs. *^{15}N in protein is expected to decrease 30% after 8 hrs and 70% after 24 hrs, mirroring the pulse experiments.*
5. After labelling, fix cells and process for MIMS as described below in **Basic Protocol 2** for correlated EM/NanoSIMS or **Alternate Protocol 1** for correlated light microscopy/NanoSIMS.

Figure 1 here

***Metabolic labelling of cell division* in vivo**

As noted above, ^{15}N-thymidine typically serves as the best label for DNA, but alternatives for studies employing multiple labels include ^{2}H-thymidine and ^{13}C-thymidine (Steinhauser et al., 2012; Kim et al., 2014; Senyo et al., 2013; Guillermier et al., 2017; Liu et al., 2019). Additionally, oral $^{2}H_2O$ has been used in human studies requiring long labelling periods (e.g., 4 weeks) (Guillermier et al., 2017a). ^{2}H is incorporated into nuclear DNA and washes out of other macromolecules (with the exception of lipids) within a few days, producing relatively specific labelling of DNA (Guillermier et al., 2017a). ^{15}N-thymidine has good bioavailability and can be administered by injection, by osmotic pump, or by mouth (e.g., in drinking water). The length of the labeling period will ultimately depend on the cell population studied, with the goal of obtaining enough labeled nuclei in the tissue section for analysis. A rapidly dividing cell population needs only a short labelling period (hours), but a rarely dividing population may require weeks to months of labeling. Likewise, a tissue with large cells (e.g., white fat) will require a longer labeling period than a tissue with more compact cells (e.g., lymph node) to capture enough labelled nuclei in the tissue section for analysis.

1. Dissolve ^{15}N-thymidine in dH2O to make a stock solution at a concentration of 20 mg/mL under a laminar flow hood. Depending on the weight of the animal, accurate administration of stock solution may necessitate a low volume syringe (e.g. Hamilton). Alternatively, calculate the total mass required for all mice being injected and dilute the stock solution further to enable accurate administration with an insulin syringe (*e.g.to* 2.5mg/ml).
2. By intraperitoneal injection, administer ^{15}N-thymidine (20 μg/g) twice daily for 3 days. *For a 25 g adult mouse, 200 μL of 2.5 mg/mL (e.g. 500 μg) ^{15}N-thymidine is injected with each dose. Doses in the range of 5 – 40 mg/kg/day have been used successfully to detect nuclei with DNA that replicated during the pulse. At this concentration, labelled nuclei have $^{15}N/^{14}N$ ratios approximately 150% above natural abundance. Labeling periods of several weeks are necessary for slowly dividing cardiac cells and adipocytes but estimates of cell renewal from more rapidly dividing cells (e.g., tumor cells and small intestinal crypt cells) can be obtained labelling periods as short as 24 hrs. Alternatively, ^{15}N-thymidine can be administered by osmotic pump or in drinking water*.

3. After metabolic labelling the mouse, perfuse and further process as described below in **Basic Protocol 2** for correlated EM/MIMS or **Alternate Protocol 1** for correlated light microscopy/MIMS.

Figure 2 here

SUPPORT PROTOCOL 1: **Preparing Silicon Wavers as Sample Supports for MIMS**

Silicon wafers are typically used to support the sample for biological MIMS analysis. Most often semi-thin sections (~500 nm) of embedded cells or tissue are captured on the silicon support, as sectioning gives access to the interior of the cell without lengthy sputtering and presents a flat surface for analysis. However, cells can be directly cultured on the silicon wafer, facilitating, e.g., analysis of the plasma membrane (Frisz et al., 2013). Additionally, smears of tissues and cells have been formed on the silicon wafers, and sperm samples have been spin cast onto the silicon support using a Headway Research spinner (Lechene et al., 2012). As an alternative to silicon wafers, TEM grids have been used as a support for ultrathin sections. This approach allows TEM and MIMS to be performed on the same section, allowing more precise TEM-MIMS registration necessary for some applications (Lovrić et al., 2017). However, ultrathin sections used for TEM are not ideal for MIMS analysis as they are fragile to presputtering and limit material available for analysis. Where possible, we routinely use adjacent ultrathin and semithin sections for TEM-MIMS correlation. Other compatible supports include metal-coated polymer filters (typically used for microbial cells from soil samples) and indium tin oxide (ITO) coated glass (Legin et al., 2014; Proetto et al., 2016).

Materials:

Silicon water 100 mm diameter (Purewafer) custom cut into squares 4.950 mm^2

Magnetic stir plate

Wire mesh strainer

4 X clean 600 mL glass beakers

4 X magnetic stir bars

Acetone

Methanol

Isopropranol

Sterile Petri dish

0.2 mm-filtered distilled water

0.2 mm-filtered EtOH

Teflon tipped forceps

Dry, filtered Nitrogen or Argon gas

Note: acetone, methanol, isopropranol are toxic and flammable. They should be stored in a safety cabinet in accordance with your institution's SOP. Steps with these chemicals should be performed with appropriate personal protective equipment (PPE) in a biosafety cabinet, following the manufacturer's SDS.

1. Place square silicon chips in a wire mesh strainer and transfer into a beaker (*e.g.* 600 mL) containing a magnetic stir bar. Completely submerge the silicon chips in acetone and wash the chips with moderate stirring for 30 min. *Handle the chips with care so as to avoid scratching the shiny surface, for example with a Teflon tipped forceps. Avoid stirring too vigorously as this may fracture chips.*
2. Transfer the strainer containing the chips to a clean 600 mL beaker containing a magnetic stir bar. Add ~250 mL of methanol to submerge the chips. Completely submerge the silicon chips in methanol and wash the chips with moderate stirring for 30 min.
3. Transfer the strainer containing the chips to a clean 600 mL beaker containing a magnetic stir bar. Add ~250 mL of isopropanol to submerge the chips. Completely submerge the silicon chips in methanol and wash the chips with moderate stirring for 30 min.
4. Remove the strainer containing the silicon chips, rinse them with 0.2 mm-filtered distilled water, and then place the strainer into a clean 600 mL beaker containing a magnetic stir bar. Completely submerge the chips in ddH_2O and wash for 30 min with moderate stirring.
5. Transfer silicon chips to a clean Petri dish. Submerge the chips in 0.2 mm-filtered EtOH. Using Teflon tipped forceps, flip the chips so that the mirror (shiny) sides are all facing up.
6. Using the Teflon tipped forceps, transfer chips into a fresh Petri dish. Dry mirrored surfaces with dry, filtered Nitrogen or Argon gas. Silicon chips are now ready to use as support for sample sections.

BASIC PROTOCOL 2: **Embedding Samples for Correlative TEM and MIMS with Genetically Encoded Reporter**

MIMS is compatible with most materials embedded for standard transmission electron microscopy (TEM). Most often Epon 812 is used as the embedding media, which offers excellent ultrastructural preservation. LR White is an alternative if additional immunostaining is planned for the sample and is discussed further below in **Alternate Protocol 1**. For correlative TEM and MIMS, we have generally used adjacent ultrathin (80 nm) and semi-thin (200 – 500 nm) sections, picked up on TEM grids and silicon chips, respectively, so that the kissing surfaces are face up. However, as an alternative, TEM and MIMS can be performed on the same ultrathin section supported by a standard TEM grid (Saka et al., 2014). Osmium tetraoxide is usually included as lipid fixative and heavy metal stain for

samples intended for correlative TEM-MIMS. Osmium tetraoxide deposition can also be detected by MIMS in the $^{16}O^-$ image to identify intracellular membranes of mitochondria, endoplasmic reticulum, and the nuclear envelope (Narendra et al., 2020).

The genetically encoded EM reporter, APEX2, can be visualized by both TEM and MIMS (Narendra et al., 2020). APEX2 is a small (250 residue) peroxidase, which locally polymerizes DAB in the presence of H_2O_2 (Lam et al., 2015; Martell et al., 2012). Polymerized DAB, in turn, binds reduced osmium tetraoxide, leading to electrodense deposits immediately around APEX2. Osmium in these APEX2 deposits can be directly measured by MIMS. Additionally, osmium has a matrix effect leading to enhanced ionization of $^{12}C^{14}N$ in the vicinity of APEX2 (Narendra et al., 2020). This is useful as it allows visualization of APEX2, while simultaneously following incorporation of ^{15}N-labelled metabolites. Similar to GFP, APEX2 can be fused to the N-terminus, C-terminus, or internal to a protein of interest. In principle, any stain utilizing DAB chemistry could be detected by MIMS in a similar manner, including horseradish peroxidase-based immunohistochemistry and histochemical stains, such as cytochrome *c* oxidase activity staining.

Materials:

1X sodium cacodylate buffer (100 mM sodium cacodylate with 2 mM Ca_2Cl, pH 7.4)

EM grade glutaraldehyde 2% (diluted in sodium cacodylate buffer from 8% glass vials) (EMS cat no: 16019)

EM Grade Paraformaldehyde (PFA) 4% (diluted in 1X PBS from 16% glass vials) (EMS cat no: 1574)

3,3'-diaminobenzidine (DAB) (Sigma, cat #D8001-10G)

Hydrogen peroxide (H_2O_2) (Sigma, cat #216763-100ML)

TAAB 812 (epon) Premix Kit Medium (TAAB, cat# T031)

1X PBS

Ethanol at 100% and diluted in dH20 to 50%, 70%, and 95% solutions

1% Osmium tetraoxide (OsO_4) diluted from 2% in H_2O (75633-2ML)

1.5% Potassium cyanide (KCN) (Sigma, 60178-25G)

Oven adjustable to 60°C

Ultramicrotome with diamond blade.

Triton-X100 (Sigma, Cat# 1086431000)

Bovine Serum Albumin (BSA)

Plasmid containing APEX2 fusion gene (Optional)

Transfection reagent such as Fugene HD (Promega, Cat# E2311) (Optional)

Note: The fixatives glutaraldehyde and PFA are toxic. Similarly, OsO_4, KCN, and DAB are toxic. Steps using these chemicals should be performed with appropriate personal protective equipment (PPE) in a biosafety cabinet, following the manufacturer's SDS. Ethanol is flammable and should be stored in anappropriate safety cabinet in accordance with your institution's SOP.

1. Seed approximately 100,000 HeLa cells in the border wells of a 24 well plate. *The small well size minimizes reagents but is still easily manipulated in the embedding process. Only the wells on the edge of the plate are used to allow access with a jeweler's saw after embedding*.
2. The next day, transiently transfect the cells with a APEX2-fusion protein (for instance Mito-APEX2 to label mitochondria), following the Fugene HD protocol. *This step can be omitted if not performing labelling with an APEX fusion protein. As an alternative to transient transfection, a stable cell line can be generated expressing a APEX2-fusion protein).*
3. Metabolically label cells with stable isotope tracers, if desired, following **Protocol 1** above.
4. Remove media, briefly wash adherent cells with pre-chilled 1X in sodium cacodylate buffer, and fix cells using pre-chilled 2% glutaraldehyde in 1X sodium cacodylate buffer at 4°C for 30 min – 1 hr. Limit fixation to 1 hr, and immediately perform labelling steps below, as APEX2 will lose peroxidase activity over time following fixation. *If APEX2 labelling is not being used, cells can be left in fixative at 4°C until embedding steps below. They are stable in fixative for months or longer. Fixation steps should be performed under a chemical hood.*

APEX2 Labelling of cells expressing APEX2-fusion proteins

5. Rinse cells with 1X sodium cacodylate buffer 3 times for 5 min each on ice.
6. During rinses, make fresh DAB staining solution by adding 1.4 mM DAB and 1 mM H_2O_2 to 1X cold sodium cacodylate buffer.
7. Add DAB staining solution to the sample and incubate at room temperature for 5 – 20 minutes, monitoring for formation of a brown DAB precipitate by transmission light microscopy. *Alternatively, DAB polymerization can be performed on ice, but may require longer incubation times (30 – 60 min). Although the reaction proceeds slower, APEX2 may retain greater peroxidase activity at 4°C. Browning due to DAB polymerization is easier to appreciate by bright field than phase contrast*.
8. After DAB precipitation, wash cells with 3 exchanges of 1X sodium cacodylate buffer for 5 min each on ice.
9. Refix cells with 2% glutaraldehyde in 1X sodium cacodylate buffer for at least 24 hrs. *Cells are stable in fixative for months or longer. Fixation steps should be performed under a chemical hood.*

Mouse tissue preparation

1. Anethetize the mouse for terminal procedure following the IACUC approved SOP of your institution and standard protocols for cardiac perfusion.
2. Whole animal perfusion with 4% PFA (with 2% glutaraldehyde if TEM is also to be performed) provides optimal tissue fixation. This is commonly performed with direct

puncture of the left ventricle after excision of the right atrium. When the heart is the target tissue, however, the perfusion step should be omitted. Instead, the beating heart is surgically exposed and removed by transecting the major vessels with scissors. While still beating, place heart in an excess of 1X PBS in a petri dish. Allow the heart to pump blood out of its chambers into the 1X PBS.

3. Dissect tissues into specimens that are ~1-2 mm^3, unless there are specific anatomic features that need to be preserved. For example, the heart can then be cross-sectioned into slices (2-3mm thick) and fixed in 2% glutaraldehyde with 4% PFA in sodium cacodylate buffer at 4°C O/N. When orthogonal immunostaining is planned for adjacent sections, use PFA alone.

Sample embedding in Epon 812 for Correlative EM-NanoSIMS Imaging

4. Osmicate the sample with reduced 1% OsO_4/ 1.5% KCN for 30 minutes. *Osmication step, dehydration, and embedding should be performed under a chemical hood.*
5. Wash sample 5 times with dH_2O.
6. Dehydrate sample using a graded series (50%, 70%, and 95%) of cold ethanol washes (diluted in dH_2O) each for 5 minutes. Wash sample in 100% ethanol three times, for 20 minutes each.
7. Remove ethanol and wash twice in propylene oxide (PO) for 15 minutes.
8. Add PO mixed 1:1 with TAAB (Epon) 812 resin kin for 1 hour.
9. Incubate sample with 100% TAAB (Epon) 812 resin kit with a few drops of PO overnight.
10. Place sample in oven preheated to 60°C for 24 hours to cure the resin.
11. For cultured cells, cut out a small resin block in the region of interest using a jeweler's saw. Trim the block further with a razor to form a trapezoid block face. An asymetrically shaped block face can be useful as each corner of resulting sections will be distinct. These distinct corners help orient the adjacent TEM and NanoSIMS sections relative to each other (even if the TEM section has been inadvertently flipped).
12. Section the block on a ultramicrotome with alternating thin (80 nm) and thick sections (500 nm) in pairs. Pick up paired thin and thick sections on a TEM grid and a silicon wafer, respectively, so that the kissing surfaces face up. *As only first few nm materials are typically analyzed from the thick section by NanoSIMS, the top surface will be closest in z-plane to the thin section analyzed by TEM. It is important that the section not be mounted near the edges of the silicon chip.*

Figure 3 here.

ALTERNATE PROTOCOL 1 : **Embedding Samples for Correlative Light Microscopy and MIMS**

MIMS has been successfully combined with light microscopy of the same or adjacent semi-thin sections, with modifications to the sample fixation and embedding protocol above. Successful applications include correlation with fluorescent dyes (Legin et al., 2014; Proetto et al., 2016), immunofluorescence (IF) (Senyo et al., 2013; Saka et al., 2014), histochemical staining (e.g., Periodic Acid Schiff and Trichrome) (Senyo et al., 2013), and fluorescent *in situ* hybridization (Senyo et al., 2013; Vujic et al., 2018). Although this protocol focuses on embedding-based methods to achieve light-MIMS correlation, an alternative approach is to grow the cells on ITO coated glass, which is compatible with light microscopy. The samples can then be dehydrated and analyzed by MIMS on

the ITO glass support without embedding (Proetto et al., 2016). We have focused on MIMS of semi-thin sections, as sectioning provides quick access to the cell interior, is generalizable to both cells and tissue, and minimizes surface topology for analysis.

For IF, fixation is usually with paraformaldehyde or formaldehyde, as glutaraldehyde blocks most antigens. Depending on the antibody, however, the addition at 0.05 – 0.2% glutaraldehyde with or without 0.2% picric acid may be tolerated and improve ultrastructure. Osmium tetraoxide should be avoided as it stains the sample black and interferes with most other colorimetric and fluorescent stains.

After fixation, the sample is typically embedded in the hydrophilic resin LR White. LR White represents a compromise between the harder but less porous (and more auto-fluorescent) Epon 812 and paraffin wax, which is too soft for ultramicrotome sectioning and performs poorly in NanoSIMS analysis. Freeze-substitution, while theoretically appealing, has been reported to give inconsistent results (Saka et al., 2014). Whereas the use of LR White comes at the cost of some reduced ultrastructural integrity (appreciable by TEM), the difference is not apparent at the lateral resolution (~30 nm) currently achievable by NanoSIMS and super-resolution light microscopy.

IF can be performed either pre- or post-embedding. Pre-embedding may be preferred for cultured cells, as antibody penetration can be limited by the LR white embedding medium and light imaging may be performed on the same section analyzed by MIMS. For pre-embedding IF, permeabilization with detergents such as Triton-X100 (at a concentration of 0.1 – 0.5%) is typically employed. As these detergents remove lipids from the sample, however, ultrastructure is disrupted (apparent by TEM) and some MIMS analyses (e.g., of lipid metabolism) may be altered. Permeabilization by other methods such as methanol or successive freeze-thaw cycles are alternatives but generally lead to greater cellular deformation (Saka et al., 2014). Alternatively, cultured cells can be embedded and sectioned prior to IF as is typically done with tissues.

IF and other staining in tissues is typically performed post-embedding, with exposure of antigen provided by sectioning. A semi-thin section (~500 nm) typically adjacent to the section analyzed by MIMS is stained. Generally, when staining LR White embedded tissue sections, higher antibody concentrations (typically starting at 1:100) and incubation times (usually doubled) are required compared to standard protocols of paraffin or cryo- sections, as penetration into the LR White embedded section is limited.

Materials:

EM Grade Paraformaldehyde (PFA) 4% (diluted in 1X PBS from 16% glass vials) (EMS cat no: 1574)

LR White Embedding Media

BEEM embedding capsule size 3 (small) (EMS, cat#69910-01)

1X PBS

Ethanol at 100% and diluted in dH20 to 50%, 70%, and 95% solutions

Oven adjustable to 60°C

Ultramicrotome with diamond blade.

Mouse tissue preparation

1. Anethetize the mouse for terminal procedure following the IACUC approved SOP of your institution and standard protocols for cardiac perfusion.
2. Whole animal perfusion with 4% PFA provides optimal tissue fixation (glutaraldehyde should be omitted). This is commonly performed with direct puncture of the left ventricle after excision of the right atrium. When the heart is the target tissue, however, the perfusion step should be omitted. Instead, the beating heart is surgically exposed and removed by transecting the major vessels with scissors. While still beating, place heart in an excess of 1X PBS in a petri dish. Allow the heart to pump blood out of its chambers into the 1X PBS.
3. Dissect tissues into specimens that are ~1-2 mm^3, unless there are specific anatomic features that need to be preserved. For example, the heart can then be cross-sectioned into slices (2-3mm thick) and fixed in 2 4% PFA in 1 X PBS buffer at 4°C O/N.

Sample embedding in LR White for Correlative Light-MIMS Imaging

1. Dehydrate the sample using a graded series (50%, 70%, and 95%) of cold ethanol washes (diluted in dH_2O) each for 5 minutes. Then, wash sample in 100% ethanol three times, for 20 minutes each. *An alteration to this step in which the sample is only partially dehydration with 2% phosphotungstic acid in 70% ethanol prior to infiltration has been reported to improve ultrastructure and antigenicity. Additionally, treatment with 1% tannic acid prior to dehydration may further improve ultrastructure and antigenicity* (Sakai et al., 2005).
2. Mix LR white resin 1:1 with 100% ethanol and add directly to the dehydrated sample. Allow resin to infiltrate the the sample overnight at 4°C.
3. The next (3^{rd}) day, for tissue samples, embed the sample in undiluted LR white resin in a BEEM embedding capsule.
4. Place sample in an oven preheated to 60°C for 24 hours to cure the resin.
5. Trim the resin embedded block into a trapezoid.
6. Section the block on a ultramicrotome at a thickness of 0.5 mm. *We routinely use 0.5 mm sections for NanoSIMS but have analyzed 0.2 to 1 mm sections by NanoSIMS with good results.*
7. Pick up adjacent sections on a silicon wafer for NanoSIMS analysis and a glass slides for light microscopy.
8. Treat section on glass slide as needed for immunohistochemistry or histochemical staining. *Note: when testing staining conditions, LR white embedded samples typically require higher antibody concentrations (e.g. 2-10X that needed for paraffin-embedded or frozen sections) and longer incubation times as the LR White resin limits reagent penetration into the sample.*

BASIC PROTOCOL 3: **Analysis of MIMS data**

More groups prepare samples for MIMS than perform MIMS, as the instruments are available in only a few centers and their operation ideally requires expertise in applied physics. Still, a basic understanding of MIMS data acquisition is helpful for planning experiments, preparing samples, and communicating experimental objectives with the MIMS center. In this section, we discuss choice of ions for analysis. We then present a detailed protocol on the analysis of MIMS data using OpenMIMS 3.0, an ImageJ/FIJI plug-in. OpenMIMS is freely available from https://github.com/BWHCNI/OpenMIMS/wiki/Installation. Alternative software packages for analysis of MIMS data include WinImage (CAMECA) and L'Image (L. R. Nittler, Carnegie Institution of Washington).

In a typical metabolic MIMS experiment, seven ions are chosen for analysis (Figure 2). These include rare atoms in the metabolic tracers, together with common elements in the sample to provide cellular and histological context. For measuring stable isotopes, two channels are needed: one tuned to the element's heavy isotope and the other to its light isotope. For instance, to detect ^{13}C-leucine and ^{15}N-thymidine stable isotope labels in a sample concurrently, an analytical configuration could include: ^{12}C, ^{13}C, ^{12}C^{14}N, and ^{12}C^{15}N. From these, two isotope ratios could be calculated, ^{13}C/^{12}C, ^{12}C^{15}N/^{12}C^{14}N. Carbon isotope ratios can also be captured by measuring ^{13}C^{14}N/^{12}C^{14}N or ^{13}C^{12}C/^{12}C$_2$.

In addition to the label atom(s), common elements within the sample are acquired to provide cellular and histological contrast. ^{12}C^{14}N, ^{31}P, and ^{32}S typically provide the best contrast, as they are abundant and differentially distributed throughout the sample, allowing delineation of cellular and histological structures.

^{12}C^{14}N and ^{32}S readily differentiate the cytosol of each cell from the nucleus and the extracellular space. Lipid-rich structures, such as lipid droplets, also stand-out as ^{12}C^{14}N holes with retained ^{12}C and ^{16}O signal. Lipid structures can be further differentiated by their ^{31}P abundance: phospholipids are ^{31}P rich and neutral lipids ^{31}P deplete. ^{31}P is typically most abundant in the nucleus, which can be further segmented into the ^{32}S-intense nucleolus and ^{32}S-sparse nucleoplasm. Within the cytoplasm, ^{32}S is enriched in some (but not all) lysosomes, providing some definition for intracellular vesicles (Legin et al., 2014, 2016; Narendra et al., 2020). Additionally, in some tissues, such as the heart and kidney, mitochondria stand out from the surrounding myofibrils, as ^{31}P-rich structures, although this is not seen in all tissues (He et al., 2018). ^{32}S is useful in defining cell types in many tissues. It is enriched in the secretory granules of Paneth cells in the intestinal crypt and granulocytes within a blood smear (Guillermier et al., 2017). Additionally, ^{32}S is highly concentrated in some extracellular structures such as in the basement membrane of the kidney, where it helps identify the glomerulus, and in the myelin sheath that envelops peripheral nerves (Legin et al., 2016).

In the addition to these contrasts intrinsic to the sample, the experimenter can introduce elements that are otherwise rare in the sample to provide further contrast. As discussed above, these include halogenated probes metabolically incorporated into DNA, lysosomes, or mitochondria: detected as Br, Fl, or Cl. Additionally, the specimen can be labelled with antibodies or oligonucleotide probes

conjugated to halogenated fluorescent dyes or metals (e.g., gold or lanthanides). Osmium tetraoxide, which binds and fixes membranes, can likewise be directly detected by MIMS as ^{192}Os or ^{16}O. Osmium deposition can also be directed by genetically encoded APEX2-fusion proteins to serve as a sort of "GFP" for MIMS. Finally, as osmium tetraoxide locally enhances ionization of high abundance ions in biological material, it can be indirectly detected as a local increase in ions such as $^{12}C^{14}N$ and ^{16}O.

Materials:

Protocol steps—*Step annotations:*

1. If multiple images have been captured as a mosaic of tiles, these can be stitched together using the "mosaic_nrrd" script. This and other manipulations to the ".im" file in OpenMIMS are saved as a ".nrrd" file.
2. Open either ".im" or ".nrrd" files in OpenMIMS. Typically, successive image planes have been captured as a stack. Summing these images increases signal, but for best results they first need to be co-registered using the "Autotrack" function.
3. To autotrack, click on the $^{12}C^{14}N$ window to make it active. Then, in the "Stack Editing" tab, click the "Autotrack" button. OpenMIMS will play through the stack one or more times during the alignment. The co-registration is automatically applied to the other ion image stacks. After autotracking, click the "Compress" button to collapse each of the ion stacks into a single image (the "Sum" button will do the same for the active window only). Each pixel in this image now equals the sum of all the co-registered pixels in the stack.

Generating a Hue Saturation Intensity (HSI) Image

We typically display isotope data as Hue Saturation Intensity (HSI) images, in which isotope ratios are represented by pixel hue and the (denominator) isotope counts by pixel intensity. Isotope counts give cellular context and differentiate areas with rich data from areas with limited data.

4. To generate an HSI image click on the "Process" tab in OpenMIMS (Figure 4A, #1). Some ratios are suggested as defaults, but additional ratios can be added to selection window using the "Add" button (Figure 4A, #2). In the selection window, highlight the desired ratio to display as an HSI image. Once highlighted, press the "Display HSI" button (Figure 4A, #3). This will generate a new window with the HSI image representing the desired isotope ratio.
5. Next, set the "Ratio Range." Note: a default scale factor of 10,000 is applied in "Ratio (scale factor)", such that the natural abundance of $^{12}C^{15}N$, 0.37%, appears as 37. Set the lower bound of the "Ratio Range" to the natural abundance (Figure 4A, #4). This renders the natural abundance blue in the HSI image. Set the upper bound of the "Ratio Range" to maximize contrast between structures with different isotope ratios. We typically choose an upper bound that is a multiple of the natural abundance, so that the scale can be expressed as the percentage of natural abundance. In Figure 4A, for example, the lower bound was set at 37 and the upper bound at 518 (Figure 4A, #5; thus, the upper bound is 1400% of natural abundance.

6. If desired, adjust the look up table for pixel intensity using the “RGB Max” and “RGB Min” sliders. In the example in Figure 4A, the default values are kept.
7. Finally, if desired, select the “Median Filter Ratio” radio button to apply a non-linear filter that removes noise. This may help define edges of structures with distinct isotope ratios or ion intensities. Again, in the example in Figure 4A the default values are kept. *All of the manipulations described in steps 5 -7 change the appearance of the HSI image to highlight features of the data but importantly do not change the underlying ion counts or isotope ratio values.*

Measuring ROIs

8. Using the “MIMS ROI Manager,” draw ROIs in the ion images showing the desired structures. For instance, in Figure 4B, lysosomes expressing Lamp1-APEX2, shown in Figure 4B appear as punctate enhancements in the $^{12}C^{14}N$ image. A circular ROI is placed within each and assigned to a lysosomal “Group” (Figure 4B, #1). Circular ROIs from the cytosol and nucleus are then selected and added to two additional “Groups.” All ROIs to be measured are selected in the “ROI Manager”. For applications where the observer is identifying cellular structures based on stereotypical, yet qualitative features, consider blinding the observer to sample and/or the labeling data (*e.g.* HSI ratio images).
9. To measure the ROIs, click on the “Tomography” tab. Select the desired “Statistics” to apply in the first window. In the middle window, select the masses to be measured. Note: if an HSI ratio image has been generated, as described, it will also appear as an available mass in the middle window. We typically measure isotope ratios from this HSI ratio image, as opposed to separately measuring the average $^{12}C^{14}N$ and $^{12}C^{15}N$ values for each ROI and then calculating a ratio. Either method is acceptable, and the calculated ratios will be similar. However, these methods are not identical. In the first case, ratios for each pixel are calculated and the ratios are then averaged across the ROI, whereas, in the second, the values of each isotope are first averaged across the ROI and then divided to obtain the ratio value for the ROI.
10. Click on the “Table” button to generate a table in the output window. The table has a column for each statistic applied to the selected masses and a row for each ROI. Additional identification columns give the file, ROI group, ROI tag, and ROI names. This output can be saved in FIJI as a comma separated values file (“.csv”) to be analyzed elsewhere. In Figure 4B, data from these ROIs have been graphed using Prism (Figure 4C).

Figure 4 here

COMMENTARY

BACKGROUND INFORMATION:

Georges Slodzian developed NanoSIMS as a form of imaging secondary ion mass spectrometry (SIMS) that optimizes spatial resolution (Slodzian et al., 1992). Multi-isotope imaging mass spectrometry (MIMS) was proposed as a general term to refer to techniques encompassing the same

principles as the original NanoSIMS prototype, particularly when combined with stable isotope tracer methods for biological applications, and is the one we have adopted in this protocol (Lechene et al., 2006). Additional terms capturing the same principles include NanoSIMS with stable isotope probing (Nano-SIP) and stable isotpe labeling kinetics and nanoscale secondary ion mass spectrometry (SILK-SIMS) (Pett-Ridge and Weber, 2012; Wildburger et al., 2018).

Unlike direct imaging SIMS techniques, which operate more like wide field light microscopy, MIMS probes one microvolume of the sample at a time, similar to a point scanning confocal microscope. This means that resolution is limited primarily by how narrow the primary ion beam can be focused on the sample. It also means that signal can be increased in principle by lengthening the dwell time at each position. To further optimize signal, MIMS operates in the dynamic mode, in which all chemical bonds of the material are broken into atoms. This reduces the number of ionic species in the microvolume while increasing the abundance of each remaining. Consequently, information is lost (e.g., the molecular origin of a particular atom within the microvolume), but signal is improved. NanoSIMS also uses multiple detectors in parallel (4 in Slodzian's prototype), each of which is kept tuned to a single species throughout the acquisition. This maximizes signal while still allowing multiple species to be compared. This also enables accurate isotope ratio measurements, as two detectors can measure the isotopes of a single element in parallel. For instance, Slodzian and colleagues initially used their prototype instrument to demonstrate that nucleolar accumulation of ^{15}N adenine could be detected as increased $^{12}C^{15}N$ signal co-localizing with ^{32}S rich nucleoli in human breast cancer cells.

MIMS is similar to several alternative techniques, but no other technique combines its high spatial resolution (down to ~30 nm lateral resolution) with high mass accuracy. Metabolic imaging by MIMS is conceptually similar to electron microscopy (EM) auto-radiography, in that both techniques follow incorporation of isotope labelled probes into cells and animal tissues at nano-scale resolution *in situ*. Although the resolution is ten-fold lower than EM autoradiography, MIMS has several advantages: (1) it uses stable isotopes rather than radioactive tracers greatly improving safety of labeling and analysis, (2) three or more metabolic tracers can be followed in parallel, (3) MIMS allows quantitative assessement of label incorporation over a larger dynamic range than *in situ* auto-radiography, (4) MIMS may be more sensitive for some applications, and (5) nitrogen, which has no radioactive isotope, can be used as a tracer in MIMS but not autoradiography.

There are also alternative mass spectrometry approaches to measure isotope ratios, but currently no alternative allows measurement at submicron resolution. Like MIMS, thermal ionization MS measures isotope ratios with high accuracy, but is limited to bulk sample analysis. LC-MS/MS can be used to measure incorporation of stable isotopes into peptides and other macromolecules but is similarly limited to bulk sample analysis. Finally, MIMS is distinct among other forms of imaging MS, such as imaging MALDI-TOF and TOF-SIMS, for its superior resolution and accurate isotope ratio measurements. However, unlike MIMS, these other imaging mass spectrometry methods allow identification of specific peptides or lipids based on their *m*/*z* ratios. This is because these methods generally operate in static rather than dynamic mode; energy applied to the sample does not completely break chemical bonds, leaving, e.g., peptides intact. A consequence of the static mode is decreased signal, which, in turn, decreases lateral resolution, as a larger microvolume must be probed in static mode to equal the signal produced in dynamic mode.

CRITICAL PARAMETERS:

A common limitation in a metabolic MIMS experiment is imaging time, with minutes to hours needed to cover a square imaging field, with dimensions ranging from 10 X 10 μm to 50 X 50 μm. Analysis time for an experiment is ultimately the product of the total area that must be imaged and the counting time required at each position for a reliable signal. Thus, minimizing these two parameters is key to maximizing usable data. Let's consider the first: the area that must be imaged. This can be reduced in at least three ways:

1. Identify structures of interest prior to NanoSIMS analysis. Identifying structures in correlated images decreases instrument time occupied by imaging dead-space or features that are not directly relevant to the hypothesis. It is important to note that unlike a light microscope or electron microscope, one cannot rapidly scan the sample with NanoSIMS for visualization. It is the actual measurements that enables the generation of high-resolution quantitative mass images. The NanoSIMS is configured with a CCD camera that allows visualization of larger landmarks, such as the contours of the section and certain anatomic features (e.g. blood vessels); however, in many instances some other form of correlative microscopy is required for identification of structures of interest prior to NanoSIMS analysis. Imaging of adjacent sections by light microscopy (e.g., a section stained with toluidine blue or immunofluorescence) or electron microscopy may provide a map of biological features of interest together with larger landmarks that can also be identified in the CCD imaging mode. Careful imaging of the region of interest in the correlated image at degressive magnifications and then mapping the whole section at low magnification is critical to finding the correlated region for NanoSIMS analysis. Another approach involves correlative imaging of the section mounted for NanoSIMS analysis, in which case x-y coordinates of discrete features of interest can be recorded for subsequent retrieval upon introduction of the sample to the NanoSIMS, using coordinate transformation. DIC and scanning electron microscopes have both been used for such applications.

2. Modify the stable isotope labeling protocol to generate more events of interest per area. One advantage of stable isotopes is their favorable toxicity profile, allowing for indefinite labeling periods. For a dichotomous labeling variable (e.g., by labeling of cell division with ^{15}N-thymidine), the effective frequency of labeled nuclei is a major determinant of requisite instrument time.

3. Concentrate the structure of interest into a smaller area (e.g., if mitochondria are the target for analysis, isolate and concentrate mitochondria prior to embedding/sectioning).

The counting time at each position can also be reduced with careful planning or iterative modifications to the analytical protocol. The counting time needed for reliable statistics depends on the ion's abundance, its ionization efficiency, and its background level in the sample. The bottleneck for each analysis will be whichever ion requires the greatest counting time. Often this will be a rare element in the sample (e.g., the gold in an immunogold labelling experiment). Omiting rare and poorly ionizing elements from the experiment can substantially reduce analysis time. Similarly, use of a stable isotope label with a higher SNR, e.g., ^{15}N over ^{13}C, can cut analysis time in half or more. Finally, maximizing labelling will ultimately reduce the counting time needed for statistical assessment.

TROUBLESHOOTING:

Common Problems	Potential Solutions
My tracer is not detectable over background in a cell culture labeling experiment?	Signal of a metabolic tracer depends on the SNR of the labelled atom in the tracer and the concentration of the metabolite incorporated into the fixable biomass of the sample. If possible, use a label with a higher SNR, e.g., ^{15}N is typically better than ^{13}C. Also, try increasing incorporation of the metabolite (e.g., by increasing its concentration, eliminating a competing unlabeled metabolite in the media or food, and/or lengthening the labelling period).
My tracer is not detectable over background in an *in vivo* labeling experiment?	The absence of detectable tracer in a target of interest could indicate that the process under investigation is very slow, and thus, reflects the underlying biology. Alternatively, it could be due to inadequate label dose or delivery. To rule out a problem with label dose or delivery, it is helpful to have a positive control. This may include assessment of labelling in a reliably active tissue (e.g. small intestine) or a catabolic output in the urine or blood. Detecting successful delivery of ^{15}N-thymidine to mice, for example, can be assessed by measuring $^{15}N/^{14}N$ isotope ratio in urine samples with bulk isotope ratio mass spectrometry analysis.
Poor ionization efficiency due to charging of the sample surface?	Since biological samples are generally not conductive, some samples may absorb the charge of the primary ion beam without resultant efficient ionization of surface material. This may be exacerbated if there is poor contact with the silicon support (e.g. wrinkles or poor adherence of section). As such, there can also be sample to sample variability in the degree of charging. There are different approaches to mitigating the effects of charging. Application of a thin layer of conductive material—i.e. gold coating the sample—can greatly improve the stability of ionization. When there is a compelling reason not to add gold (e.g. immunogold labeling), in some instances we have prepared multiple redundant samples and then selected the sample that empirically has the

	best ionization properties.
Cells or structures of interest imaged by TEM cannot be found by NanoSIMS.	Correlating TEM with MIMS can be challenging. The same cells imaged by TEM needs to be located in the adjacent MIMS section on an opaque support by reflection DIC light microscopy, which provides lower contrast than transmission light microscopy. To orient the NanoSIMS section to the TEM section image, it is helpful if the sections have an asymmetric shape (achieved by cutting the cell/tissue block face into an asymmetric trapezoid prior to sectioning). It is also helpful to choose cells of interest that are near one of the corners of the section or at least near the edge of the section. The cells of interest should be imaged at the desired resolution by TEM and then at progressively lower magnifications to show their location in the section. The whole section should then be mapped at the lowest resolution by TEM and then assembled into a map with the location of target cells indicated.

UNDERSTANDING RESULTS:

^{15}N-leucine labelled HeLa cells chased in unlabeled leucine for 24 hrs show puncta with retained ^{15}N-leucine. These puncta are a subset of lysosomes with decreased protein turnover relative to the cytosol and nucleus. Identification of these puncta as lysosomes is established in several ways: (1) they co-localize with the lysosomal marker Lamp1-APEX2, detected as focal enhacement in the $^{12}C^{14}N^-$ image; (2) they correspond to lysosomes in the correlated TEM image; and (3) they co-localize with $^{32}S^-$-rich cytosolic puncta, the vast majority of which are lysosomes (Figure 2, bottom right, arrow).

Do the higher $^{15}N/^{14}N$ ratios in these puncta really reflect differences in bulk protein turnover? Two control experiments convince us they do. The protein translator cycloheximide blocks ^{15}N increase in the sample, proving that incorporation of the label (i.e., ^{15}N) corresponds to incorporation of intended target metabolite (i.e., new protein). Second, a label switch experiment (light → heavy rather than heavy → light) produces the inverse pattern of labelling: most lysosomes now have decreased rather than increased $^{12}C^{15}N^-/^{12}C^{14}N^-$ ratios relative to cytosol (Narendra et al., 2020). Thus, differences in label ratio ($^{12}C^{15}N^-/^{12}C^{14}N^-$) reflects differences in metabolite turnover and not an experimental artifact.

In experiments conducted with ^{15}N-thymidine, the goal is typically to determine the frequency of ^{15}N-labeled nuclei. In the first analysis, ^{15}N-thymidine labeled nuclei are treated as a dichotomous variable, similar to how BrdU-labelled nuclei are treated in light microscopy-based methods. In many instances, the high-resolution mass images reveal morphological and elemental features that identify cell types of interest. For example, cardiomyocyte nuclei are identifiable by their association

with intracellular sarcomeric structures. Likewise, adipocyte nuclei are identifiable by their association with intracellular lipid droplets. A blinded observer identifies all nuclei in a cell population of interest, and calculates the frequency of ^{15}N positive cells in that population. Once such nuclei are selected, the absolute isotope ratios for the nuclei can also be extracted from the imaging files. These quantitative data provide another layer of analysis in a pulse-chase experiment, as cell turnover can also be assessed as a 50% dilution of label with each cell division. Thus, cells that have divided once during the pulse (and have 50% label) can be differentiated from cells that have divided twice (and have 25% label).

TIME CONSIDERATIONS:

Basic Protocol 1: Metabolic Labelling for NanoSIMS

Pulse labelling cells. 8 - 24 hrs.

Chase labeling cells. 5 days pulse followed by 1 day chase.

In vivo labelling of dividing nuclei. 1 day to 6 weeks.

Support Protocol 1: Preparing Silicon Wavers as Sample Support for NanoSIMS

1 day.

Basic Protocol 2: Embedding Samples for Correlative TEM and NanoSIMS with Genetically Encoded Reporter

Transfecting cells with APEX-fusion protein. 2 days.

Fixation and processing for EM. 5 days.

Alternative Protocol 1: Embedding Samples for Correlative Light Microscopy and NanoSIMS

Fixation and processing for EM. 5 days.

Basic Protocol 3: Analysis of NanoSIMS data

1 – 3 days.

ACKNOWLEDGEMENTS: (mandatory for NIH, optional for all others)

This research was supported in part by the Intramural Research Program of the National Institutes of Health, National Institute of Neurological Disorders and Stroke; extramural National Institutes of Health (grant DP2-CA216362), the Brigham and Women's Hospital Department of Medicine Evergreen Innovation Award.

LITERATURE CITED:

Angelo, M., Bendall, S. C., Finck, R., Hale, M. B., Hitzman, C., Borowsky, A. D., Levenson, R. M., Lowe, J. B., Liu, S. D., Zhao, S., et al. 2014. Multiplexed ion beam imaging of human breast tumors. *Nature Medicine* 20:436–442.

Behrens, S., Lösekann, T., Pett-Ridge, J., Weber, P. K., Ng, W.-O., Stevenson, B. S., Hutcheon, I. D., Relman, D. A., and Spormann, A. M. 2008. Linking Microbial Phylogeny to Metabolic Activity at the Single-Cell Level by Using Enhanced Element Labeling-Catalyzed Reporter Deposition Fluorescence In Situ Hybridization (EL-FISH) and NanoSIMS. *Applied and Environmental Microbiology* 74:3143–3150.

Ducker, G. S., Chen, L., Morscher, R. J., Ghergurovich, J. M., Esposito, M., Teng, X., Kang, Y., and Rabinowitz, J. D. 2016. Reversal of Cytosolic One-Carbon Flux Compensates for Loss of the Mitochondrial Folate Pathway. *Cell Metabolism* 23:1140–1153.

Frisz, J. F., Lou, K., Klitzing, H. A., Hanafin, W. P., Lizunov, V., Wilson, R. L., Carpenter, K. J., Kim, R., Hutcheon, I. D., Zimmerberg, J., et al. 2013. Direct chemical evidence for sphingolipid domains in the plasma membranes of fibroblasts. *Proceedings of the National Academy of Sciences of the United States of America* 110:E613-622.

Guillermier, C., Fazeli, P. K., Kim, S., Lun, M., Zuflacht, J. P., Milian, J., Lee, H., Francois-Saint-Cyr, H., Horreard, F., Larson, D., et al. 2017a. Imaging mass spectrometry demonstrates age-related decline in human adipose plasticity. *JCI Insight* 2. Available at: https://insight.jci.org/articles/view/90349 [Accessed May 13, 2020].

Guillermier, C., Poczatek, J. C., Taylor, W. R., and Steinhauser, M. L. 2017b. Quantitative imaging of deuterated metabolic tracers in biological tissues with nanoscale secondary ion mass spectrometry. *International Journal of Mass Spectrometry* 422:42–50.

Guillermier, C., Steinhauser, M. L., and Lechene, C. P. 2014. Quasi-simultaneous acquisition of nine secondary ions with seven detectors on NanoSIMS50L: application to biological samples. *Surface and interface analysis: SIA* 46:150–153.

He, C., Weston, T. A., Jung, R. S., Heizer, P., Larsson, M., Hu, X., Allan, C. M., Tontonoz, P., Reue, K., Beigneux, A. P., et al. 2018. NanoSIMS Analysis of Intravascular Lipolysis and Lipid Movement across Capillaries and into Cardiomyocytes. *Cell Metabolism* 27:1055-1066.e3.

Keren, L., Bosse, M., Thompson, S., Risom, T., Vijayaragavan, K., McCaffrey, E., Marquez, D., Angoshtari, R., Greenwald, N. F., Fienberg, H., et al. 2019. MIBI-TOF: A multiplexed imaging platform relates cellular phenotypes and tissue structure. *Science Advances* 5:eaax5851.

Kim, S. M., Lun, M., Wang, M., Senyo, S. E., Guillermier, C., Patwari, P., and Steinhauser, M. L. 2014. Loss of white adipose hyperplastic potential is associated with enhanced susceptibility to insulin resistance. *Cell Metabolism* 20:1049–1058.

Lam, S. S., Martell, J. D., Kamer, K. J., Deerinck, T. J., Ellisman, M. H., Mootha, V. K., and Ting, A. Y. 2015. Directed evolution of APEX2 for electron microscopy and proximity labeling. *Nature Methods* 12:51–54.

Lechene, C., Hillion, F., McMahon, G., Benson, D., Kleinfeld, A. M., Kampf, J. P., Distel, D., Luyten, Y., Bonventre, J., Hentschel, D., et al. 2006. High-resolution quantitative imaging of mammalian and bacterial cells using stable isotope mass spectrometry. *Journal of Biology* 5:20.

Lechene, C. P., Lee, G. Y., Poczatek, J. C., Toner, M., and Biggers, J. D. 2012. 3D multi-isotope imaging mass spectrometry reveals penetration of 18O-trehalose in mouse sperm nucleus. *PloS One* 7:e42267.

Lechene, C. P., Luyten, Y., McMahon, G., and Distel, D. L. 2007. Quantitative imaging of nitrogen fixation by individual bacteria within animal cells. *Science (New York, N.Y.)* 317:1563–1566.

Legin, A. A., Schintlmeister, A., Jakupec, M. A., Galanski, M., Lichtscheidl, I., Wagner, M., and Keppler, B. K. 2014. NanoSIMS combined with fluorescence microscopy as a tool for subcellular imaging of isotopically labeled platinum-based anticancer drugs. *Chemical Science* 5:3135–3143.

Legin, A. A., Theiner, S., Schintlmeister, A., Reipert, S., Heffeter, P., Jakupec, M. A., Mayr, J., Varbanov, H. P., Kowol, C. R., Galanski, M., et al. 2016. Multi-scale imaging of anticancer platinum(iv) compounds in murine tumor and kidney. *Chemical Science* 7:3052–3061.

Liu, H., Zhang, C.-H., Ammanamanchi, N., Suresh, S., Lewarchik, C., Rao, K., Uys, G. M., Han, L., Abrial, M., Yimlamai, D., et al. 2019. Control of cytokinesis by β-adrenergic receptors indicates an approach for regulating cardiomyocyte endowment. *Science Translational Medicine* 11.

Lovrić, J., Dunevall, J., Larsson, A., Ren, L., Andersson, S., Meibom, A., Malmberg, P., Kurczy, M. E., and Ewing, A. G. 2017. Nano Secondary Ion Mass Spectrometry Imaging of Dopamine Distribution Across Nanometer Vesicles. *ACS nano* 11:3446–3455.

Martell, J. D., Deerinck, T. J., Sancak, Y., Poulos, T. L., Mootha, V. K., Sosinsky, G. E., Ellisman, M. H., and Ting, A. Y. 2012. Engineered ascorbate peroxidase as a genetically-encoded reporter for electron microscopy. *Nature biotechnology* 30:1143–1148.

Narendra, D. P., Guillermier, C., Gyngard, F., Huang, X., Ward, M. E., and Steinhauser, M. L. 2020. Coupling APEX labeling to imaging mass spectrometry of single organelles reveals heterogeneity in lysosomal protein turnover. *The Journal of Cell Biology* 219.

Nuñez, J., Renslow, R., Cliff, J. B., and Anderton, C. R. 2017. NanoSIMS for biological applications: Current practices and analyses. *Biointerphases* 13:03B301.

Pett-Ridge, J., and Weber, P. K. 2012. NanoSIP: NanoSIMS applications for microbial biology. *Methods in Molecular Biology (Clifton, N.J.)* 881:375–408.

Proetto, M. T., Anderton, C. R., Hu, D., Szymanski, C. J., Zhu, Z., Patterson, J. P., Kammeyer, J. K., Nilewski, L. G., Rush, A. M., Bell, N. C., et al. 2016. Cellular Delivery of Nanoparticles Revealed with Combined Optical and Isotopic Nanoscopy. *ACS nano* 10:4046–4054.

Saka, S. K., Vogts, A., Kröhnert, K., Hillion, F., Rizzoli, S. O., and Wessels, J. T. 2014. Correlated optical and isotopic nanoscopy. *Nature Communications* 5:3664.

Sakai, Y., Hosaka, M., Hira, Y., and Watanabe, T. 2005. Addition of phosphotungstic acid to ethanol for dehydration improves both the ultrastructure and antigenicity of pituitary tissue embedded in LR White acrylic resin. *Archives of Histology and Cytology* 68:337–347.

Senyo, S. E., Steinhauser, M. L., Pizzimenti, C. L., Yang, V. K., Cai, L., Wang, M., Wu, T.-D., Guerquin-Kern, J.-L., Lechene, C. P., and Lee, R. T. 2013. Mammalian heart renewal by pre-existing cardiomyocytes. *Nature* 493:433–436.

Slodzian, G., Daigne, B., Girard, F., Boust, F., and Hillion, F. 1992. Scanning secondary ion analytical microscopy with parallel detection. *Biology of the Cell* 74:43–50.

Steinhauser, M. L., Bailey, A. P., Senyo, S. E., Guillermier, C., Perlstein, T. S., Gould, A. P., Lee, R. T., and Lechene, C. P. 2012. Multi-isotope imaging mass spectrometry quantifies stem cell division and metabolism. *Nature* 481:516–519.

Thomen, A., Najafinobar, N., Penen, F., Kay, E., Upadhyay, P. P., Li, X., Phan, N. T. N., Malmberg, P., Klarqvist, M., Andersson, S., et al. 2020. Subcellular Mass Spectrometry Imaging and Absolute Quantitative Analysis across Organelles. *ACS nano* 14:4316–4325.

Vujic, A., Lerchenmüller, C., Wu, T.-D., Guillermier, C., Rabolli, C. P., Gonzalez, E., Senyo, S. E., Liu, X., Guerquin-Kern, J.-L., Steinhauser, M. L., et al. 2018. Exercise induces new cardiomyocyte generation in the adult mammalian heart. *Nature Communications* 9:1659.

Wildburger, N. C., Gyngard, F., Guillermier, C., Patterson, B. W., Elbert, D., Mawuenyega, K. G., Schneider, T., Green, K., Roth, R., Schmidt, R. E., et al. 2018. Amyloid-β Plaques in Clinical Alzheimer's Disease Brain Incorporate Stable Isotope Tracer In Vivo and Exhibit Nanoscale Heterogeneity. *Frontiers in Neurology* 9:169.

FIGURE LEGENDS:

Figure 1. Metabolic imaging with MIMS. A ^{15}N-leucine labelled HeLa cell transfected with Lamp1-APEX2 was chased in light media for 24 hrs, fixed, and processed for MIMS. Within the instrument, positively-charged cesium ions from the primary source sputter a microvolume of sample, forming negatively-charged secondary ions. These are focused into a secondary ion beam and then separated by their *m/z* ratios in the magnetic sector of the instrument. Seven detectors (T1 – T7) are spaced to detect up to seven ion species in parallel. These include $^{12}C^{15}N^-$ (mass 27) and $^{12}C^{14}N^-$ (mass 26), from which a hue saturated intensity (HSI) ratio image can be calculated (dotted arrows). The hue scale on the bottom of the HSI image, ranges from 100 to 600% of ^{15}N natural abundance. Incorporation of ^{15}N-leucine into the sample is seen as an increase in $^{12}C^{15}N^-$ over its natural abundance. Other species detected in parallel, including $^{32}S^-$, provide additional contrast. In the cell expressing Lamp1-Apex2, lysosomes (arrow) appear as focal increases in $^{12}C^{14}N^-$. These lysosomes are additionally $^{32}S^-$ intense and can be detected in a transmission electron micrograph (TEM) of an adjacent section (arrow). The lysosomal membrane is dark in the TEM due to expression of Lamp1-APEX2 on the cytosolic face of the lysosomal membrane. Figure is adapted from (Narendra et al., 2020).

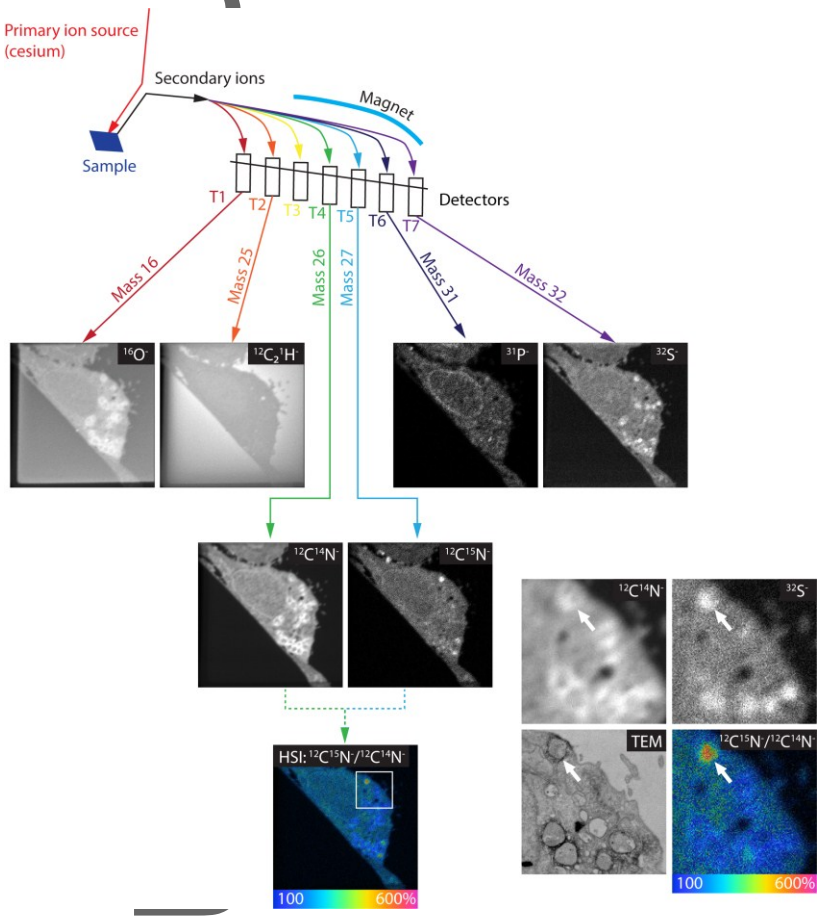

Figure 2. Analyzing dividing cells in the mouse intestinal crypt with MIMS. A male C57Bl/6 mouse was co-injected with ^{15}N-thymidine (500 ug) and ^{2}H-thymidine twice daily for three days. The animal was perfused with PFA 4% and a tissue sample was processed for MIMS as described in **Protocol 2**. MIMS analysis of an intestinal crypt was performed using a peak-switching method that allows acquistion of up to nine ions in parallel (Guillermier et al., 2014). Paneth cells at the base of the crypt are readily identified in the $^{32}S^-$ image by their sulfur-rich granules. These granules also have low $^{31}P^-$ counts (white arrows in the magnified images on bottom right). In the magnified image, nuclei of a likely crypt base columnar cell (CBC, yellow arrow), a Paneth cell (yellow arrowhead), and three enterocytes are identifiable by their high $^{31}P^-$ and low $^{32}S^-$ signals. Incorporation of ^{15}N-thymidine into these nuclei is indicated by an increased $^{12}C^{15}N^-/^{12}C^{14}N^-$ ratio in the HSI image; the three enterocytes (yellow *) and a CBC cell (yellow arrow) divided during the pulse, whereas the the Paneth cell did not (yellow arrow head). Similarly, ^{2}H-thymidine incorporation is detected as an increased ratio in the $^{12}C_2H^-/^{12}C_1H^-$ HSI image. In contrast, there is no increase in the ratio of $^{13}C/^{12}C$ over natural abundance; this is as expected as no ^{13}C-labelled probe was administered.

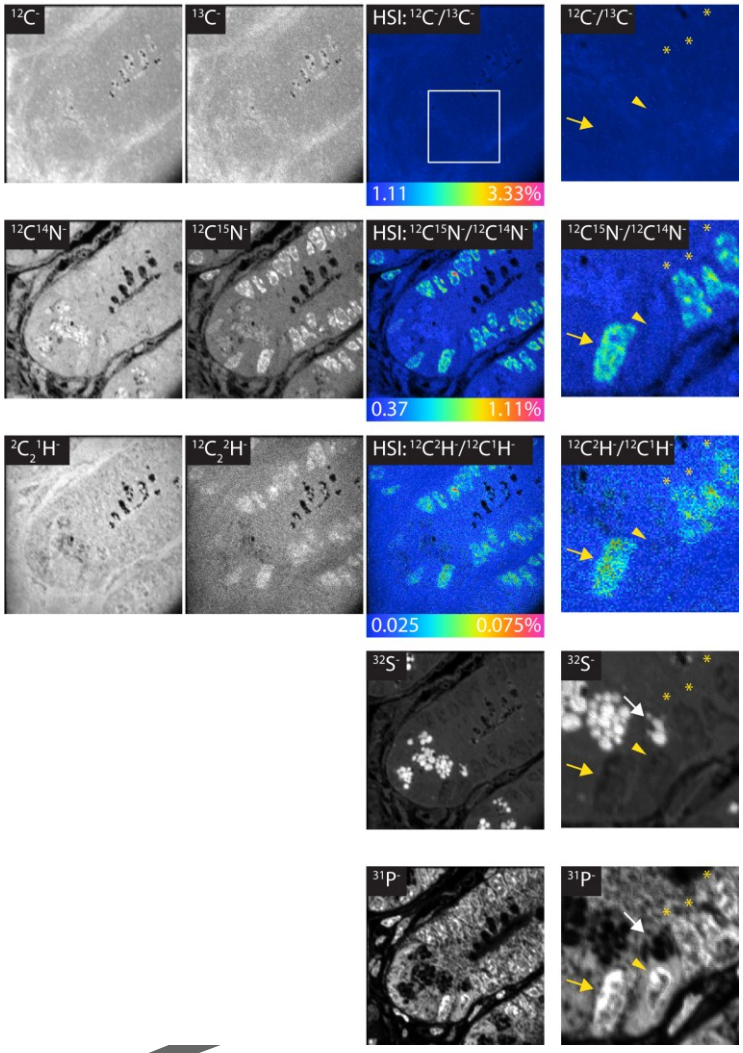

Figure 3. Correlated TEM-MIMS of cultured cells. (A) Adjacent sections from an untransfected HeLa cell were analysed by TEM (top) and analyzed by MIMS, producing $^{12}C^{14}N^-$ and $^{16}O^-$ ion images (bottom). After lipid fixation with osmium tetraoxide, membrane contrast is apparent in the $^{16}O^-$ image, allowing delineation of mitochondria (tinted green in magnification), endoplasmic reticulum (tinted purple in magnification), and nuclear envelope (tinted blue in magnification). (B) MIMS images of a HeLa cell transfected with Mito-APEX2 are shown. $^{32}S^-$ intense puncta in the upper left image are lysosomes, which are seen more clearly in the $^{32}S^-/^{16}O^-$ ratio image (bottom left, pseudo-colored magenta). The image was windowed for high ratio values and further processed in FIJI using the "despeckle" and "smooth" functions. Mito-APEX2, marking mitochondria, leads to osmium deposits in mitochondria. These are directly detected as increased $^{192}Os^-$ counts (upper right image) and indirectly as enhancement of the $^{12}C^{14}N^-$ signal (top, middle). A ratio image of fo the $^{12}C^{14}N/^{12}C$ specifically highlights the APEX2-marked mitochondria (lower middle panel, pseudo-colored green). Merge of lysosomes and mitochondria is shown in the lower right image. Figure is adapted from (Narendra et al., 2020).

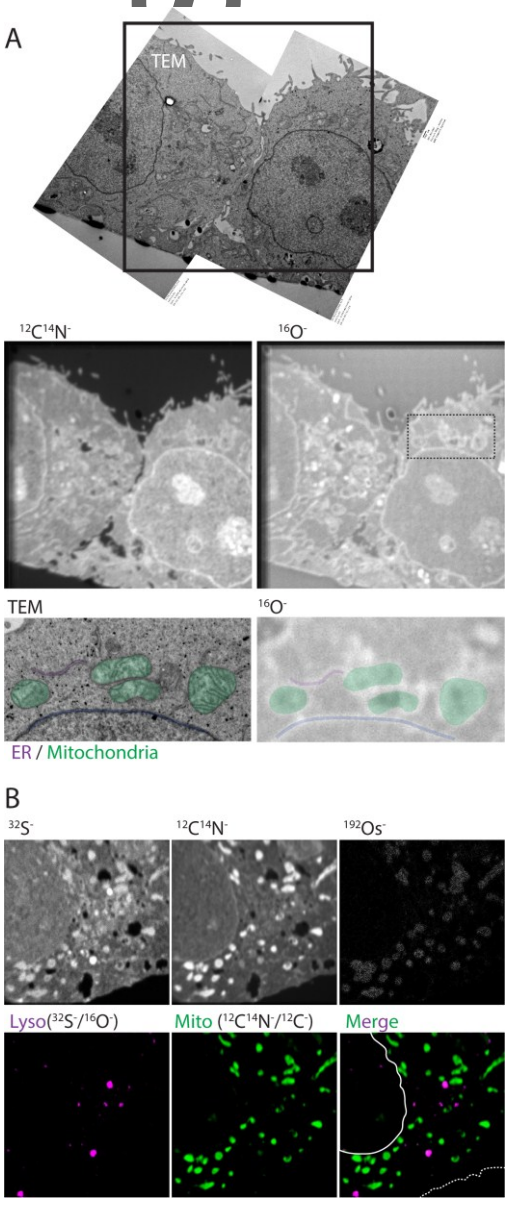

Figure 4. Analyzing MIMS data in OpenMIMS. ^{15}N-leucine labelled HeLa cells transfected with Lamp1-APEX2 were chased in light media for 24 hrs. (A) Hue saturated intensity (HSI) images of isotope ratios was generated using the "Process" tab of the OpenMIMS window (#1 in figure). A window to the left is prepopulated default ratios. Additional ratios of any two ion images can be added using the "Add" button (#2 in figure). After highlighting the desired ratio ($^{12}C^{15}N^-/^{12}C^{14}N^-$), the "Display HSI button" (#3 in figure) generates the $^{12}C^{15}N^-/^{12}C^{14}N^-$ HSI image (upper right). The hue range is set in the "Ratio Range" windows (#4 in the figure). Note: the default is to scale the ratios by 10,000 to avoid decimal points. The minimum value in the ratio range is set at 37 corresponding to the natural abundance of ^{15}N (i.e., 0.37%). The maximum value is set to a multiple of 37 that maximizes contrast in the ratio in the HSI image: in this case, 518. Thus, the maximum hue represents 5.18% ^{15}N and corresponds to 1200% of its natural abundance. (B) ROIs are selected using the MIMS ROI Manager. (C) Graph depicts $^{12}C^{15}N^-/^{12}C^{14}N^-$ measured from ROIs selected in (B). ROIs were placed within individual lysosomes from each of the cells in the field (L1, L2, and L3) and compared to cytosolic (C1, C2, and C3) and nuclear (N1 and N2) ROIs in the corresponding cells. Black line indicates the average value for each group. Dotted line is 100% of natural abundance. Figure is adapted from (Narendra et al., 2020).